

Noise Correlations and Quantum Coherence in Hard-core Bosons in One-dimensional Lattices

Ana Maria Rey [1], Indubala I Satija [2] and Charles W Clark,
National Institute of Standard and Technology, Gaithersburg MD, 20899
 (Dated: April 1, 2022)

Noise correlations, such as those observable in the time of flight images of a released cloud, are calculated for hard-core bosonic (HCB) atoms. We find that the standard mapping of HCB systems onto spin-1/2 XY models fails in application to computation of noise correlations. This is due to the contribution of *multiply occupied virtual states* to noise correlations in bosonic systems. Such states do not exist in spin models. We use these correlations to explore quantum coherence of the ground states and re-address the relationship between the peaks present in noise correlation and the Mott phase. Our analysis points to distinctive new experimental signatures of the Mott phase. The importance of these correlations is illustrated in an example of a quasiperiodic potential that exhibits a localization transition. In this case, in contrast to the momentum distribution, the noise correlations reveal the presence of quasiperiodic order in the localized phase.

In recent years, great experimental progress has been achieved in the coherent control of ultra-cold gases. In particular by loading a Bose-Einstein condensate into a tight two-dimensional optical lattice, an array of one dimensional tubes has been created [3, 4, 5, 6, 7]. Using this setup, recent experiments have been able to successfully enter the Tonks-Girardeau regime (TG) [3, 5, 6], where the strong interactions between the bosons mimic the Pauli exclusion principle [8], and to realize the Mott insulator transition in one dimension[5].

Recent theoretical and experimental studies have shown that the atomic shot noise [9, 10, 11, 12] in the time of flight images can be useful to decode various correlations underlying many-body states of trapped ultra-cold atoms. For ultra-cold bosons in a Mott insulator state, for example, these second order correlations have been proven to complement the standard, momentum-distribution based, characterization of the phase coherence. [9, 11]. Such correlations have also been used to probe pair condensation in a fermionic superfluid [10].

In this paper, we develop a theoretical framework to compute noise correlations in one dimensional hard core bosonic atoms (HCB) in a lattice. The HCB Hamiltonian is identical to that of spin-1/2 XY model which in turn can be mapped to that of spinless fermions.[13, 14] Although these three systems have identical spectra and local observable, their off-diagonal correlation functions differ. Experimentally relevant two-point correlation functions are identical for HCB and spin-1/2 systems, and the general formulation to calculate these functions was developed by Lieb and Mattis[14], based on Wick's theorem. To the best of our knowledge, this formulation has not been extended to higher order correlations. Here we complete such an extension to treat four-point correlation functions. One of the central results of this paper is the discovery of important differences between higher order correlation functions of HCB and spin-1/2 systems. The root of this difference is the fact that HCB systems have virtual states which may be multiply occupied, whereas spin-1/2 states are always at most singly occupied.

We use the noise correlations to explore quantum coherence in systems with and without an external parabolic confinement. Our analysis generalizes, to the strongly correlated

(fermionized) regime, previous studies of noise correlations carried out in the Mott insulator limit.[9, 11] We show that, *independent of the filling factor of the system*, HCB exhibits second order coherence displayed as peaks in the noise shot images which reflect the order induced by the lattice potential. This suggests that the second order coherence in noise correlations is a generic attribute of the strongly correlated regime and does not merely indicate reduced number fluctuations (This was also noted in earlier studies in a different context.[9, 12]). On the other hand, we find that the intensity of peaks depends exclusively on the relative coordinates only in Mott-insulator limit. Thus a regular pattern in the noise correlation could serve as a definitive signature of the existence of a Mott phase. Finally, we show that noise correlations are also important in describing the quantum coherence of HCB systems in the presence of quasiperiodic disorder. Quasiperiodicity induces an Anderson-type localization transition [17] in the system. In the delocalized phase, both the first and the second order correlations are found to exhibit characteristic Bragg peaks at the Fibonacci sites reflecting quasiperiodic order. However, in the localized phase only noise correlations show these peaks.

The Bose-Hubbard Hamiltonian describes bosons in optical lattices when the lattice is loaded in such a way that only the lowest vibrational level of each lattice site is occupied and tunneling occurs only between nearest-neighbor sites,[15]:

$$H = -J \sum_{\langle i,j \rangle} \hat{a}_i^\dagger \hat{a}_j + \frac{U}{2} \sum_j \hat{n}_j (\hat{n}_j - 1) + \sum_j V_j \hat{n}_j \quad (1)$$

Here \hat{a}_j is the bosonic annihilation operator of a particle at site j , $\hat{n}_j = \hat{a}_j^\dagger \hat{a}_j$, and the sum $\langle i, j \rangle$ is over nearest neighbors. The hopping parameter J , and the on-site interaction energy U are functions of the lattice depth. V_j represents any other external potential such as a parabolic confinement or on-site disorder.

In a typical experiment, atoms are released by turning off the external potentials at time $t = 0$. The atomic cloud expands, and is photographed after it enters the ballistic regime. Assuming that the atoms are noninteracting from the time of release, properties of the initial state can be inferred from the

spatial images: $\langle \hat{n}[x(t)] \rangle$, reflects the initial momentum distribution, n_q , and the image shot noise, $\mathcal{G}[x(t), x'(t)]$ reflects the momentum space fluctuations, namely the *noise correlations*, $\Delta(q_1, q_2)$,

$$\begin{aligned} \langle \hat{n}[x(t)] \rangle &\propto \langle \hat{n}_q \rangle = \sum_{n,m} e^{i\frac{2\pi}{L}q(n-m)} \langle \hat{a}_n^\dagger \hat{a}_m \rangle \\ \mathcal{G}[x(t), x'(t)] &\propto \langle (\hat{n}_{q_1} - \langle \hat{n}_{q_1} \rangle)(\hat{n}_{q_2} - \langle \hat{n}_{q_2} \rangle) \rangle \equiv \Delta(q_1, q_2) \\ &= \sum_{n,m,l,j} e^{i\frac{2\pi}{L}q_1(n-m)} e^{i\frac{2\pi}{L}q_2(i-j)} \langle \hat{a}_n^\dagger \hat{a}_m \hat{a}_l^\dagger \hat{a}_j \rangle \end{aligned}$$

where L is the number of lattice sites. In the strongly correlated regime, Eq. (1) can be replaced by the HCB Hamiltonian,

$$H - J \sum_j (\hat{b}_j^\dagger \hat{b}_{j+1} + \hat{b}_{j+1}^\dagger \hat{b}_j) + \sum_j V_j \hat{n}_j \quad (2)$$

Here \hat{b}_j is the annihilation operator at the lattice site j which satisfies $[\hat{b}_{i \neq j}, \hat{b}_j^\dagger] = 0$, and the on-site condition $\hat{b}_j^2 = \hat{b}_j^{\dagger 2} = 0$, which suppresses multiple occupancy of lattice sites. The same relations are fulfilled by Spin-1/2 raising and lowering operators. However, the exact on-site commutation relation differ between HCB and spin-1/2 operators, and this becomes important in processes involving virtual states. This distinction between spin and HCB models has not been explored in earlier studies; it has no effect on either the mapping of HCB to free fermions or on the calculations of local observable and the momentum distribution. However, the presence of multiply occupied lattice sites in virtual states that occurs in HCB strongly affects the noise correlation. A simple example of this can be seen in the computation of the correlation function, $\langle 1 | \hat{b} \hat{b}^\dagger | 1 \rangle$. In the spin-1/2 model this correlation function is zero, while for HCB it is equal to 2. On the other hand $\langle 1 | \hat{b}^\dagger \hat{b} | 1 \rangle = 1$ for both systems.

We now describe the way in which we have generalized the approach of Lieb and Mattis. We have found a simple recipe to take into account the problem of multiple occupancy of the virtual state. In our calculation of the four point correlations $\langle \hat{b}_n^\dagger \hat{b}_m \hat{b}_l^\dagger \hat{b}_j \rangle$, each occurrence of a term $\hat{b}_j \hat{b}_j^\dagger$ is replaced by the $1 + \hat{b}_j^\dagger \hat{b}_j$ (Note that no new rules are needed if we encounter number operators, $\hat{b}_j^\dagger \hat{b}_j$ or operators at different sites). In other words, only those four-point correlation functions involving two or more equal sites where the pair has the form $\hat{b}_j \hat{b}_j^\dagger$, should be treated differently from that of the corresponding spin correlations. We will refer this recipe as *multiple occupancy of virtual state rule* (MOV). The validity of MOV was checked by comparing various correlation functions obtained using the above recipe with those obtained by diagonalizing a full Bose-Hubbard Hamiltonian with a large U value.

The following procedure is used to calculate the four-point correlation functions. We first rearrange the operators so that the site index is ordered (this is only relevant for the case when three or more site indices are different); then we apply MOV; next, we use the Jordan-Wigner transformation

accordingly to the prescription of Lieb and Mattis; and finally we use Wick's theorem to write higher order correlations in terms of the free-fermionic propagators, $g_{lm} = \sum_{s=0}^{N-1} \psi_l^{*(s)} \psi_m^{(s)}$, with N being the total number of atoms and $\psi_l^{(s)}$ the s^{th} eigenfunctions of the single-particle Hamiltonian $-J(\psi_{l+1}^{(s)} + \psi_{l-1}^{(s)}) + V_l \psi_l^{(s)} = E^{(s)} \psi_l^{(s)}$. To present our results we denote the creation and the annihilation operators by b^α , where $\alpha = +1(-1)$ for annihilation (creation) operators, respectively, and the "site ordered" four-point correlation function is designated by $\chi_{abcd}^{\alpha\beta\gamma\delta}$.

$$\langle \hat{b}_n^\dagger \hat{b}_m \hat{b}_l^\dagger \hat{b}_j \rangle \mapsto \langle \hat{b}_a^{(\alpha)} \hat{b}_b^{(\beta)} \hat{b}_c^{(\gamma)} \hat{b}_d^{(\delta)} \rangle \equiv \chi_{abcd}^{\alpha\beta\gamma\delta} \quad (3)$$

In this equation it is implicit that $a \leq b \leq c \leq d$, and this order is implied in all the expressions that follow. We define $G_{ij} \equiv 2g_{ij} - \delta_{i,j}$ and $B_{ij} \equiv \langle \hat{b}_i^\dagger \hat{b}_j \rangle$. The latter can be calculated in terms of G_{ij} [14]. We introduce four matrices \mathbf{M} , \mathbf{S} , \mathbf{X} and \mathbf{Y} in terms of which our results for the correlation functions can be written. These matrices are presented at the end of this paper due to their notational complexity. Our results for the correlation functions then take the form:

$$\begin{aligned} \chi_{abbd}^{\alpha\beta\gamma\delta} &= \frac{1 - \beta\gamma}{2} \left[\frac{1}{4} |\mathbf{M}(a, b, d)| + \left(\frac{1}{2} + \delta_{\beta, -1} \right) B_{ad} \right], \\ \chi_{aacd}^{\alpha\beta\gamma\delta} &= \frac{1 - \alpha\beta}{2} \left[\frac{1}{4} |\mathbf{S}(a, c, d)| + \left(\frac{1}{2} + \delta_{\alpha, -1} \right) B_{cd} \right], \\ \chi_{abcc}^{\alpha\beta\gamma\delta} &= \frac{1 - \gamma\delta}{2} \left[\frac{1}{4} |\mathbf{S}(c, a, b)| + \left(\frac{1}{2} + \delta_{\gamma, -1} \right) B_{ab} \right], \\ \chi_{abcd}^{\alpha\beta\gamma\delta} &= (-1)^{b+d-c-a} \left[\frac{2 - \gamma\delta - \alpha\beta}{16} |\mathbf{X}(a, b, c, d)| + \right. \\ &\quad \left. \frac{\beta}{4} (\delta_{\gamma, -1} - \delta_{\alpha, -1}) |\mathbf{Y}(a, b, c, d)| \right]. \end{aligned} \quad (4)$$

When three, four or two pairs of indices are equal the calculation is rather straight forward. The non-vanishing correlation functions of this type are given by: $\langle \hat{b}_n^\dagger \hat{b}_n \hat{b}_n^\dagger \hat{b}_n \rangle = g_{nn}$, $\langle \hat{b}_n^\dagger \hat{b}_n \hat{b}_m^\dagger \hat{b}_m \rangle = g_{nn} g_{mm} - g_{nm}^2$, $\langle \hat{b}_n^\dagger \hat{b}_m \hat{b}_m^\dagger \hat{b}_n \rangle = g_{nn} g_{mm} - g_{nm}^2 + g_{nn}$ and $\langle \hat{b}_n^\dagger \hat{b}_n \hat{b}_n^\dagger \hat{b}_m \rangle = \langle \hat{b}_m^\dagger \hat{b}_n \hat{b}_n^\dagger \hat{b}_n \rangle = B_{nm}$ with $n \neq m$.

The formulas above were used in numerical calculations of the momentum distributions and the noise correlations for lattices of $L = 55$ sites and $N = 19$ atoms with periodic boundary conditions. Fig.1 shows both first and second order correlations along with the density profile. There we also include effects of a magnetic confinement $V_j = j^2 \Omega / J$ on various correlations. Experimentally the ratio Ω / J can be changed either by changing the lattice depth or the external magnetic confinement. The parameters used in our analysis relate to typical experimental set-ups such as the ones reported in ref[5].

The density profiles (Fig1a) for different values of Ω / J show that only in the case $\Omega / J = 0.17$ does the ground state of the system correspond to a Mott insulator. In this case

all the central N sites have unit filling. For $\Omega/J = 0.018$ localization takes place only at the central site, while for $\Omega/J = 0.008$ and 0 , all the sites have filling factor less than unity. The formation of a Mott state with reduced number fluctuations for $\Omega/J = 0.17$ is clearly signaled by the momentum distribution (Fig1b), which shows a flat profile. On the other hand for the other cases where number fluctuations are important, there is a clear peak in the momentum distribution at $q = 0$. This peak reflects the quasi-long-range correlations in the density matrix of these systems [16].

In contrast to the momentum distribution, the noise-correlations $\Delta(q_1, 0)$ (Fig1c) for all values of Ω/J are peaked at $q_1 = 0$. This lattice induced peak is observable due to the strong particle correlations in the fermionized regime and disappears in the weakly correlated regime where most of the atoms are Bose-condensed. In our numerical study without any confining potential, where we vary the filling factors (not shown in the figures), the central ($q_1 = 0$) peak in the noise correlations showed the same particle-hole symmetry as the central peak in the momentum distribution. The value of $\Delta(0, 0)$ increases with filling factor, ν , up to $\nu = 1/2$, and then decreases to its minimum value of $2 - 1/L$ at unit filling when the system is in the Mott phase. For partially filled states ($N < L$), the quantity $\Delta(q_1, 0)$ has a dip near $q_1 = 0$. This satellite dip disappears in the Mott phase, in which case, $\Delta(q_1 \neq 0, 0)$ is a constant equal to $-1/L$. As seen in Fig. 1, these observations remain qualitatively valid in the presence of a trap, where the analysis of the noise correlations is more complicated,

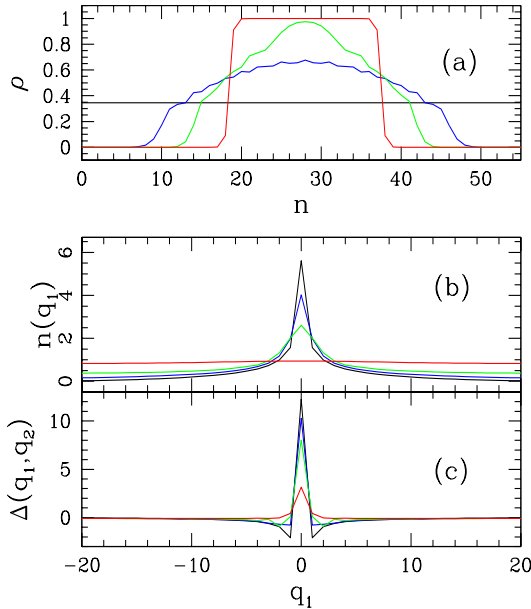


FIG. 1: Density (a), momentum distribution (b) and noise correlation (c) with different trapping potentials: $\Omega/J = 0$ (black), 0.008 (blue), 0.018 (green), 0.17 (red)). Here $q_2 = 0$, $N = 19$ and $L = 55$. For finite Ω , the correlation functions are renormalized by a scaling factor N/Z where Z are the number of sites with non-zero density.

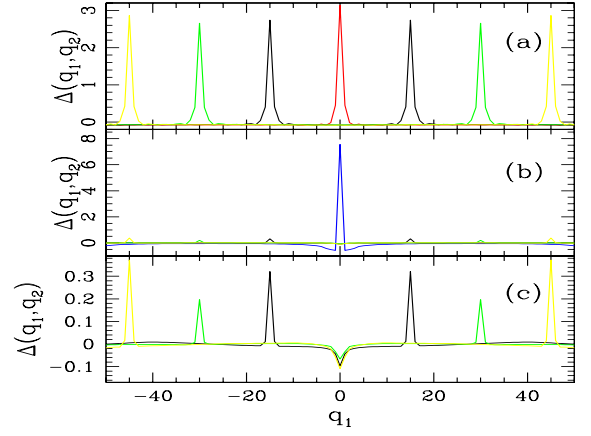


FIG. 2: Mott (a) and non-Mott(b) phase (obtained with $\Omega/J = 0.17$ and $\Omega/J = 0.008$ respectively) using $L = 55$ and $N = 19$. Each color corresponds to $\Delta(q_1, q_2)$ for a fixed q_2 as a function of q_1 . Thus different colors correspond to different values of q_2 . Peaks occur when $q_1 = q_2$. Red (blue) show the peak when $q_2 = 0$ in the Mott (non-Mott) phase. Other peaks correspond to $q_2 = 15$ (black), 30 (green), 45 (yellow). Panel (c) is a blowup of panel (b) where we show $q_2 \neq 0$ correlations only.

The existence of second order coherence in HCB systems, independent of their filling factor, implies that the peaks cannot be used as a signature of the Mott insulator in 1D systems. Nevertheless, our numerical calculations show that only when the system is a Mott insulator, the noise-correlations exhibit a regular pattern, *i.e.* $\Delta(q_1, q_2) \approx \Delta(q_1 - q_2)$ (small differences seen in Fig. 2 are due to the finite trap). Fig. 2 illustrates the contrast between the Mott (Fig2a) and the non-Mott (Fig2b-c) phase. In addition to the variation in the intensity of the peaks, the $q_2 \neq 0$ correlations show a dip at the center (Fig2c).

As a final example we introduce quasiperiodicity by adding a potential $V_j = 2\lambda \cos(2\pi\gamma j + \phi)$ where λ is an amplitude and γ is an irrational number which introduces competing periodicities in the system. We choose $\gamma = (\sqrt{5} - 1)/2$ and $\phi = \pi/4$. The free-fermion Hamiltonian with this potential exhibits localization-delocalization transition at $\lambda = 1$ [17]. In our numerical study, γ is replaced by a ratio of two Fibonacci numbers F_n/F_{n+1} , ($F_1 = F_0 = 1, F_{n+1} = F_n + F_{n-1}$), which describe the best rational approximant, obtained by continued fraction expansion of γ [17]. Here we treat the case of $\gamma = 55/89$, $L = 89$ and $N = 25$. In the extended phase ($\lambda < 1$), the spectrum is effectively continuous and the eigenstates are of the Bloch type, while in the localized phase, the spectrum is point-like and the eigenstates are exponentially localized. Because in its ground state, all the lowest N single particle levels are occupied, the HCB system displays its metal-insulator transition in the density profile: in the extended phase, the on-site density varies smoothly between sites, while in the localized phase it is discontinuous.

The effects of quasiperiodic disorder on HCB are depicted in Fig.3. We see in Fig.3a that the localization transition destroys the cusp in the central peak of the momentum distribu-

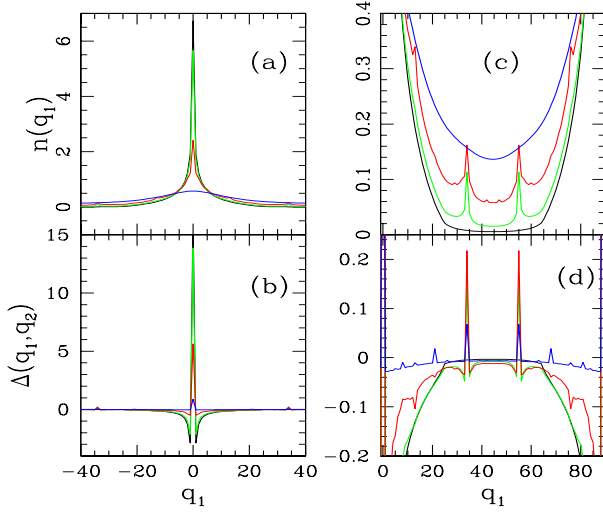


FIG. 3: Quantum coherence as quasiperiodic disorder varies: $\lambda = 0$ (black), 0.5 (green), 1 (red), 2 (blue). Figures on the right show a blowup of the Fibonacci peaks which are barely visible on the left. Additionally, distinct harmonic peaks can be seen at 68, 76, 81. (Here $q_2 = \Omega/J = 0$)

tion, demonstrating the loss of first order quantum coherence. However, second order quantum coherence is preserved, as shown in the structure of the noise correlations, Fig. 3b. This is analogous to the changes in coherence associated with the Mott transition in the absence of disorder. Additional peaks reflecting quasiperiodic order of the system appear at the reciprocal lattice vectors $\frac{2\pi}{L}F_n$ (Figs. 3c,d). The localization transition destroys these peaks in the momentum distribution (3c), yet they remain in the noise correlations (3d). In other words, in the localized phase, no trace of the quasiperiodic order remains in first order correlations, but it is still seen clearly in second order correlations. The intensities of these second order Bragg peaks increase with disorder in the extended phase and reach a maximum value at the onset to localization, after which they decrease. Furthermore, at the critical point as well as in the localized phase, we see additional structure at various harmonics of two frequencies that underly the quasiperiodicity of the system. The harmonic peaks in the localized phase reflect self-similar fluctuations of the wave function [18]. We hope that our studies of quasiperiodic quantum coherence (whose details will be published elsewhere) will stimulate experimental studies of such systems, for example in two-color optical superlattices [19].

$$\mathbf{M} = \begin{pmatrix} G_{aa+1} & G_{ab-1} & G_{ab+1} & \dots & G_{ac} \\ \vdots & & & & \vdots \\ G_{b-1a+1} & G_{b-1b-1} & G_{b-1b+1} & \dots & G_{b-1c} \\ G_{b+1a+1} & G_{b+1b-1} & G_{b+1b+1} & \dots & G_{b+1c} \\ \vdots & & & & \vdots \\ G_{c-1a+1} & G_{c-1b-1} & G_{c-1b+1} & \dots & G_{c-1c} \end{pmatrix}, \quad \mathbf{X} = \begin{pmatrix} G_{ba} & \dots & G_{bb-1} & G_{bc+1} & \dots & G_{bd-1} & G_{bc} \\ G_{a+1a} & \dots & G_{a+1b-1} & G_{a+1c+1} & \dots & G_{a+1d-1} & G_{a+1c} \\ \vdots & & & & & \vdots & \\ G_{b-1a} & \dots & G_{b-1b-1} & G_{b-1c+1} & \dots & G_{b-1d-1} & G_{b-1c} \\ G_{c+1a} & \dots & G_{c+1b-1} & G_{c+1c+1} & \dots & G_{c+1d-1} & G_{c+1c} \\ \vdots & & & & & \vdots & \\ G_{da} & \dots & G_{db-1} & G_{dc+1} & \dots & G_{dd-1} & G_{dc} \end{pmatrix}$$

$$\mathbf{S} = \begin{pmatrix} G_{aa} & G_{ab+1} & \dots & G_{ac} \\ G_{ba} & G_{bb+1} & \dots & G_{bc} \\ \vdots & & & \vdots \\ G_{c-1a} & G_{c-1b+1} & \dots & G_{c-1c} \end{pmatrix}, \quad \mathbf{Y} = \begin{pmatrix} G_{a+1a} & G_{a+1b} & G_{a+1a+1} & \dots & G_{a+1b-1} & G_{a+1c+1} & \dots & G_{a+1d-1} \\ \vdots & & & & & & & \vdots \\ G_{b-1a} & G_{b-1b} & G_{b-1a+1} & \dots & G_{b-1b-1} & G_{b-1c+1} & \dots & G_{b-1d-1} \\ G_{c+1a} & G_{c+1b} & G_{c+1a+1} & \dots & G_{c+1b-1} & G_{c+1c+1} & \dots & G_{c+1d-1} \\ \vdots & & & & & & & \vdots \\ G_{d-1a} & G_{d-1b} & G_{d-1a+1} & \dots & G_{d-1b-1} & G_{d-1c+1} & \dots & G_{d-1d-1} \\ G_{ca} & G_{cb} & G_{ca+1} & \dots & G_{cb-1} & G_{cc+1} & \dots & G_{cd-1} \\ G_{da} & G_{db} & G_{da+1} & \dots & G_{db-1} & G_{dc+1} & \dots & G_{dd-1} \end{pmatrix}$$

In the above matrices, dots indicate continuous variation of the indices. In the absence of dots, the indices are explicitly written and they may not change continuously.

[1] arey@nist.gov.

[2] Permanent address: Dept. of Phys., George Mason U., Fairfax, VA, 22030; isatija@physics.gmu.edu.

[3] B. Laburthe Tolra *et al* Phys. Rev. Lett. **92**, 190401 (2004).

[4] H. Moritz *et al*, Phys. Rev. Lett. **91**, 250402 (2003).

[5] B. Paredes *et al* Nature **429**, 277 (2004).

[6] T. Kinoshita *et al*, Science **305**, 1125 (2004).

[7] C. D. Fertig *et al*, Phys. Rev. Lett. **94**, 120403 (2005).

- [8] M. Girardeau, J. Math. Phys. **1**, 516 (1960).
- [9] E. Altman *et al*, Phys. Rev. A **70**, 013603 (2004). preprint
- [10] M. Greiner *et al* Phys. Rev. Lett. **94**, 110401 (2005)
- [11] S. Foelling *et al*, Nature **434**, 481 (2005).
- [12] L. Mathey *et al*, cond-mat/0507108 (2005).
- [13] E. H. Lieb and W. Liniger, Phys. Rev. **130**, 1605 (1963).
- [14] E. Lieb, T. Schultz and D. Mattis, Ann. Phys. 16 (1961) 407.
- [15] D. Jaksch *et al* Phys. Rev. Lett. **81**, 3108 (1998).
- [16] M. Rigol and A. Muramatsu, Phys. Rev. A **72**, 013604 (2005)
- [17] B. Simon, Adv. Appl. Math. **3**, 463 (1992).
- [18] J. Ketoja and I. Satija, Phys Rev Lett, 75, 2762, 1995.
- [19] R. Roth and K. Burnett, Phys Rev A, **68**, 023604 (2003).